Electronic Supplementary Information

Molecular dynamics simulation study of linear to bottle brush to star-like amphiphilic block polymer assembly in solution

Michiel G. Wessels[1], and Arthi Jayaraman[1,2,]*

1. 150 Academy Street, Colburn Laboratory, Department of Chemical and Biomolecular Engineering, University of Delaware, Newark, DE 19716

2. Department of Materials Science and Engineering, University of Delaware, Newark, DE 19716

*corresponding author arthij@udel.edu
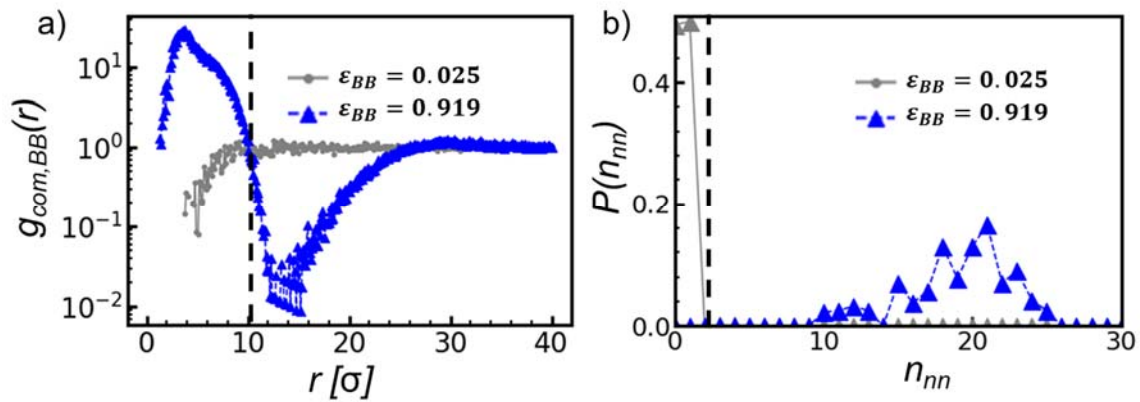
Figure S.1. Determination of parameters used to define a chain as part of a cluster. (a) *A:B* 50:50 bottlebrush (N_{bb}=24 N_{sc}=3) B-block center of mass radial distribution function at η = 0.025. The dashed line indicates the critical radius (b) Distribution of nearest neighbors for bottlebrush *A:B* 50:50 within the critical radius. The minimum number of nearest neighbors is indicated by the dashed line, in order to exclude chains in a disordered fluid-like state.
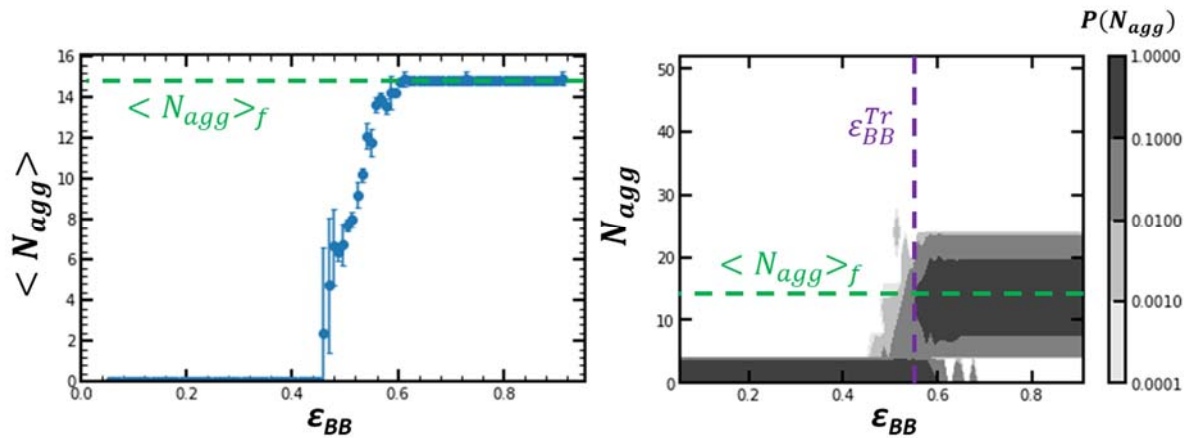
Figure S.2. *Determination of transition solvophobicity, $\varepsilon_{BB}{}^{tr}$.* (a) Aggregation number for bottlebrush *A:B* 50:50 (N_{bb}=24 N_{sc}=3) as a function of increasing solvophobicity, ε_{BB}. The dashed line indicates the plateau aggregation number, $<N_{agg}>_f$. (b) Probability distribution of N_{agg} as a function of solvophobicity. The horizontal line indicates the plateau aggregation number. The transition solvophobicity is indicated by the vertical line, where the probability of the $N_{agg}=<N_{agg}>_f$ reaches 0.1.
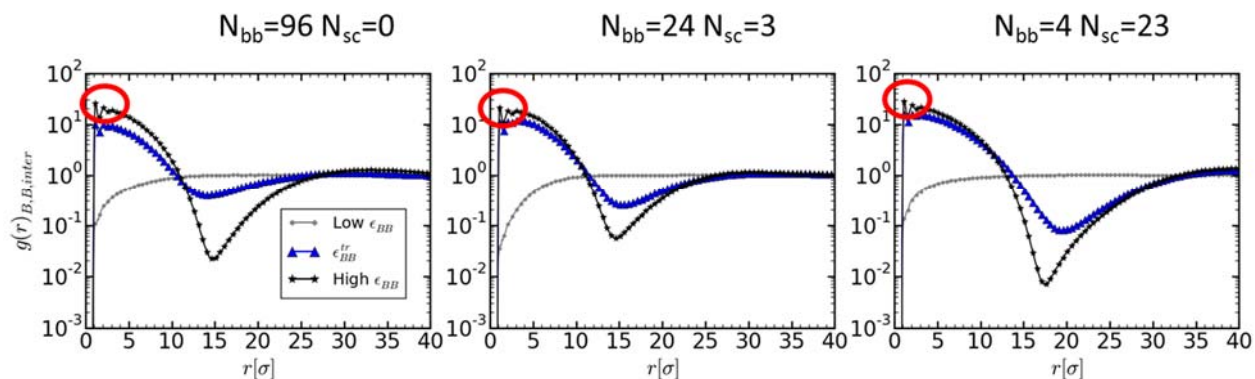
Figure S.3. Determination of 1st peak g(r)$_{B-B, inter}$ at high solvophobicity, to indicate the number of contacts within the assembled micelle for three select architectures (linear, bottle brush and star-like). Gray circles represent the radial distribution function at low solvophobicity where chains are in a randomly ordered fluid-like state. Blue triangles represent the radial distribution function at transition solvophobicity, ε_{BB}^{tr} (calculated as shown in the example in Figure S.2.). Black stars represent the radial distribution function at high solvophobicity after the micelle assembly has reached a plateau.
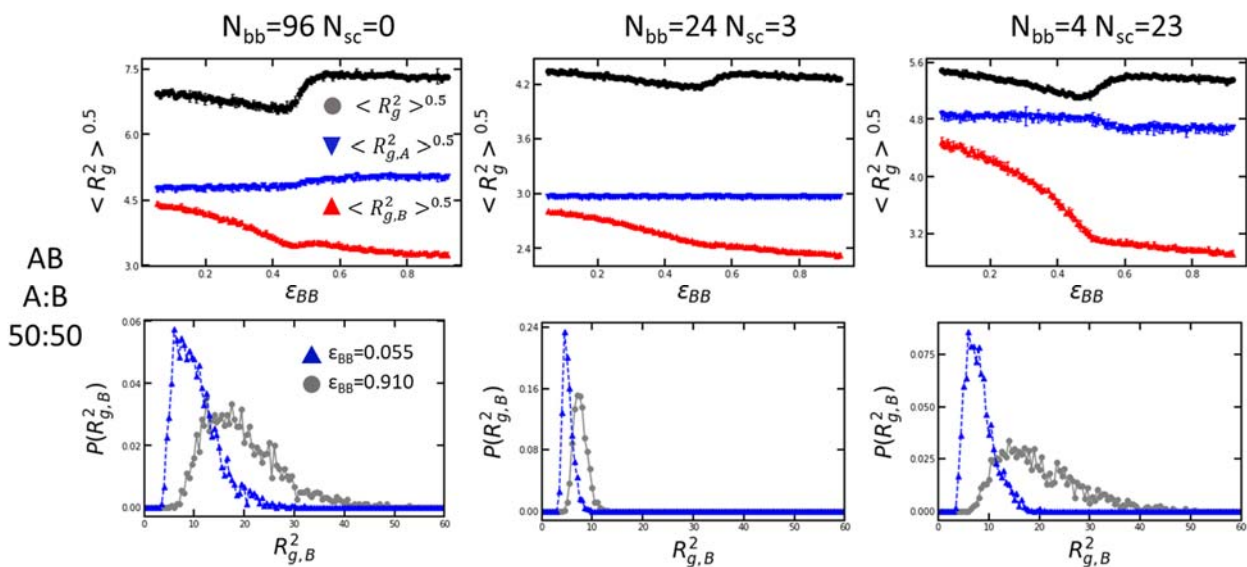
Figure S.4. (Top row) Determination of B-block chain radius of gyration as a function of increasing solvophobicity, ε_{BB}, for three select architectures (linear, bottle brush and star-like). (Bottom row) Radius of gyration probability distribution for three select architectures (linear, bottle brush and star-like), indicating the change in conformations between low solvophobicity (blue triangle) and high solvophobicity (gray circle).
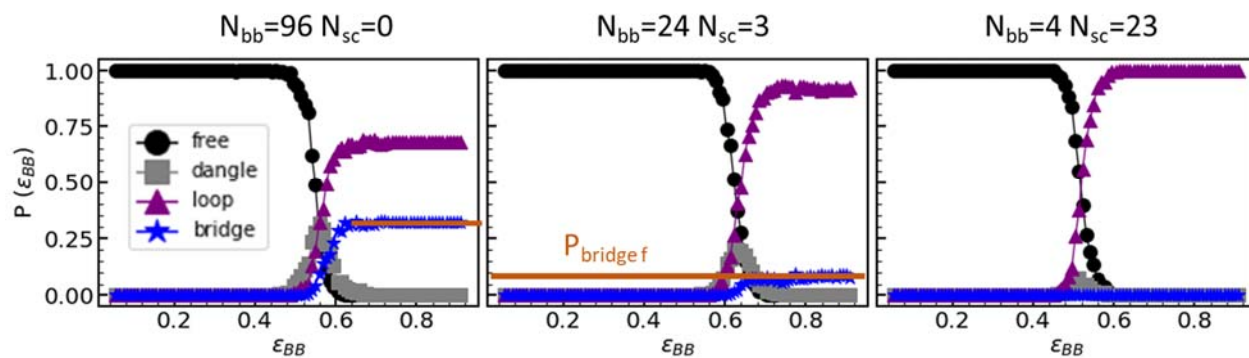
Figure S.5. *Determination final/plateau probability of bridged conformations for three select architectures (linear, bottle brush and star-like).* Indicating the evolution of different conformations with increasing ε_{BB}. Chains where both ends are free in solution (i.e. free) are indicated in black circles, chains that have one end in a micelle and the other free in solution (i.e. dangle) are indicated by gray squares, chains that have both ends in the same micelle (i.e. loop) at shown with purple triangles and chains with the two ends in different micelle cores (i.e. bridge) are shown with blue stars.

$$\text{Packing parameter } (p) = \frac{V}{l_c A}$$

$p < 1/3$ $1/3 < p < 1/2$ $1/2 < p < 1$
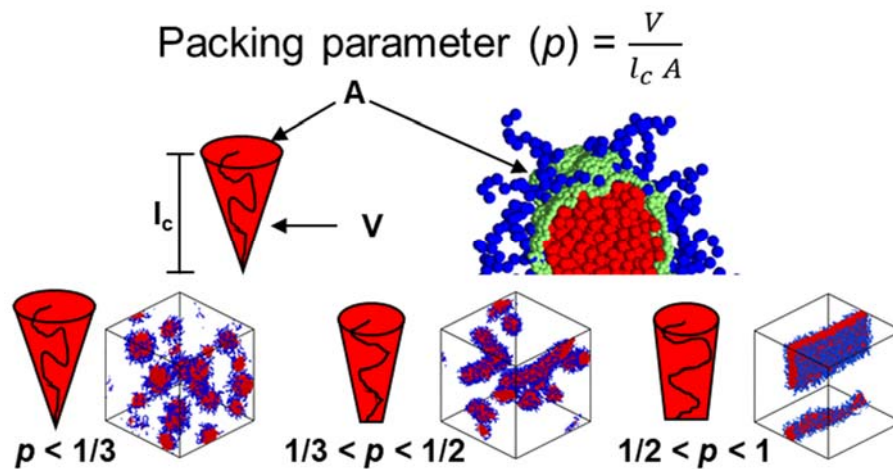
Figure S.6. Schematic of the chain packing parameter (p) calculation. Values of $p < 1/3$ indicate spherical morphologies, values between 1/3 and 1/2 indicate cylindrical morphologies, and values between 1/2 and 1 indicate bilayer-like morphologies.

(a)

1	2	3	4	5	6
$N_{bb} = 144$	$N_{bb} = 72$	$N_{bb} = 48$	$N_{bb} = 36$	$N_{bb} = 24$	$N_{bb} = 18$
$N_{sc} = 0$	$N_{sc} = 1$	$N_{sc} = 2$	$N_{sc} = 3$	$N_{sc} = 5$	$N_{sc} = 7$

7	8	9	10	11	
$N_{bb} = 16$	$N_{bb} = 12$	$N_{bb} = 8$	$N_{bb} = 6$	$N_{bb} = 4$	
$N_{sc} = 8$	$N_{sc} = 11$	$N_{sc} = 17$	$N_{sc} = 23$	$N_{sc} = 35$	

(b)
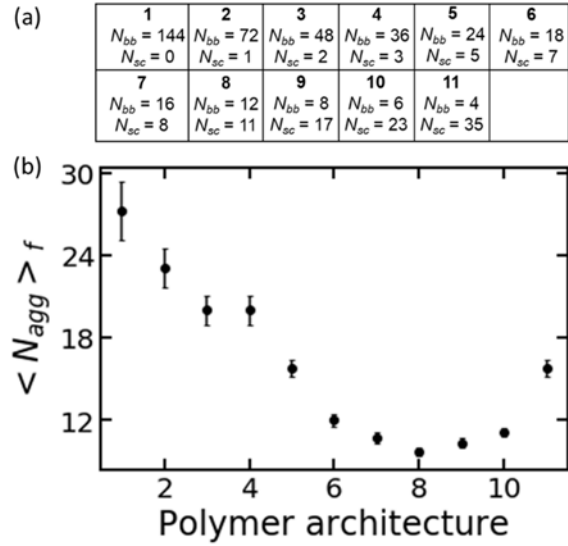
Figure S.7. Micelle structural characteristics for A:B 50:50 amphiphilic BPs and Ntot=144 of (a) varying polymer architectures and (b) the aggregation number at ε_{BB}=0.8. The error bars indicate the 95% confidence interval for the results of *one* simulation trial (unlike multiple simulation trials for the main paper results)
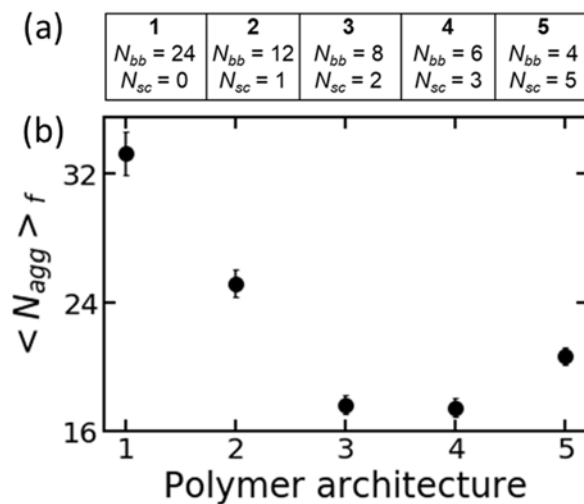
Figure S.8. Micelle structural characteristics for A:B 50:50 amphiphilic BPs and Ntot=24 of (a) varying polymer architectures and (b) the aggregation number at εBB=1. The error bars indicate the 95% confidence interval for the results of *one* simulation trial (unlike multiple simulation trials for the main paper results)

To verify that the first peak of the intermolecular B-B radial distribution function is a representative quantity of the energetically favorable intermolecular contacts within the micelle core and that this value is not significantly affected by the different number of B beads at the micelle surfaces for different polymer architectures as their micelle sizes differ, we consider a second approach to calculate number of energetically favorable intermolecular contacts. For this second approach, we want to focus on only the interior of the micelle core. To identify the interior of the micelle core, we use concentration profiles plotted with increasing distance from the micelle center of mass in **Figure S.9**.
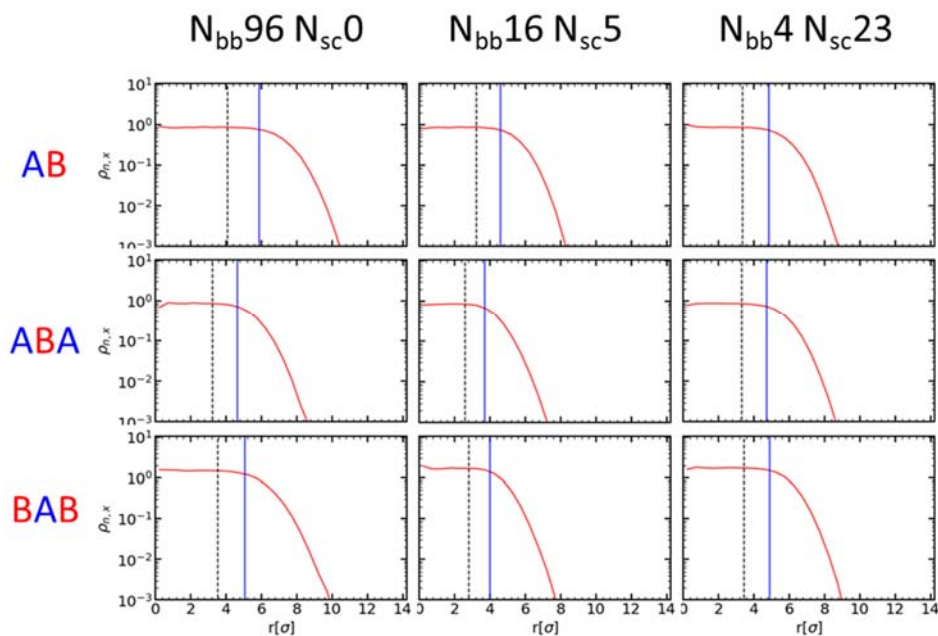
Figure S.9. Number density, $\rho_{n,x}$, profiles from the micelle center of mass for different polymer architectures and block sequences. The solid red line indicates the total number density of B-beads, $\rho_{n,B}$. The vertical solid blue line indicates the average micelle core radius of gyration and the vertical dashed black line indicates 70% of the average core radius of gyration.

From **Figure S.9.** we see that the micelle core radius of gyration is close to the core-corona interface, where the bead number density starts to decrease. In order to exclude the core-corona interface we

consider only B beads within 70% of the core radius of gyration to calculate the number of intermolecular B-contacts within the micelle core.
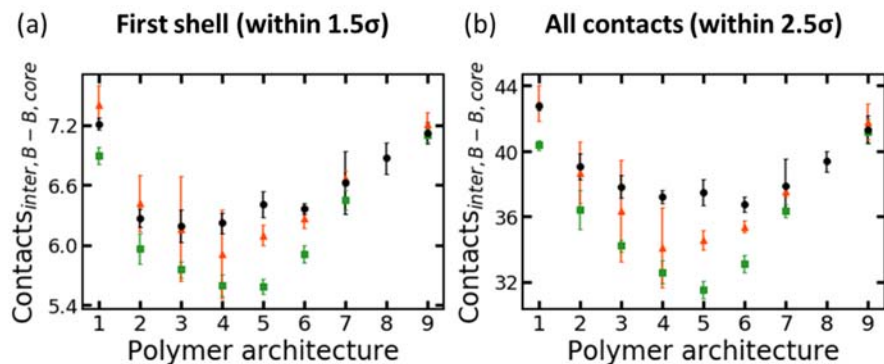
Figure S.10. Intermolecular B-B bead contacts in the micelle core (within 70% of the core radius of gyration from the micelle center of mass) for different polymer architectures and block sequences. (a) shows intermolecular B-B contacts within 1.5σ and (b) within 2.5σ.

The trends from **Figure S.10.** closely match the trends in **Figure 2f** indicating that excluding beads at the core-corona interface does not significantly impact the number of energetically favorable intermolecular B-B contacts within the micelle core. We also tested the sensitivity of the results to the 70% criteria and found that the qualitative trends do not change whether even with 50% of the micelle core radius of gyration as a cut-off criterion (data not shown).
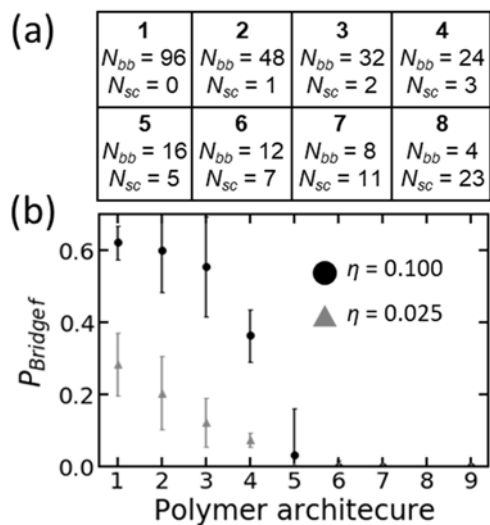
Figure S.11. Polymer bridging characteristics for (a) varying polymer architectures with BAB block sequence. (b) Final (plateau) probability for a chain to bridge two micelles of A:B 50:50 composition for two different polymer occupied volume fractions. The error bars indicate the 95% confidence interval between the results of three independent simulations.